Gyroscope based floating LIDAR design for getting stable offshore wind velocity profiles

Kameswara Sridhar Vepa[a], Thomas Duffey[b], and Wim Van Paepegem[a]
[a] Mechanics of Materials and Structures, Ghent University, Zwijnaarde, Belgium.
[b] 3E Headquarters, Brussels, Belgium.

***Abstract*—This letter focuses on a stabilization mechanism for a floating LIght Detection And Ranging (LIDAR) device that helps in taking accurate wind velocity profiles for offshore wind mills. The 3E company headquartered in Brussels developed a buoy on which the LIDAR has to be mounted. Goal is to study the response of the 3E prototype buoy in comparison to the PEM58 buoy (commercial modular constructed buoy) for response to the incoming waves and suggest a stabilization mechanism to compensate for the movements of the buoy. A gyroscope based approach is implemented for the stabilization mechanism. Commercially available kinematic simulation software – Universal Mechanism (UM) is used to simulate the kinematics of the mechanism. Two buoy models are simulated viz., 3E prototype and PEM58 in a numerical wave tank using coupled Finite element (FE) - Smoothed Particles Hydrodynamics (SPH) method. Wave tank generated waves are used to assess the movements of the buoys. These movements of the buoys are applied to the stabilization mechanism and the displacements of the LIDAR module are recorded. It is shown that the gyroscope based stabilization mechanism performs well for recording measurements accurately by keeping the LIDAR module parallel to the undisturbed free surface.**

***Index Terms* — Floating LIDAR, Smoothed Particle Hydrodynamics (SPH), Stabilization mechanism, Gyro mechanism.**

I. INTRODUCTION

Offshore wind power is achieving greater prominence and is evolving very fast in the current energy market. One key factor driving the performance of offshore wind energy is the wind profile which gives wind velocity and direction distribution at a particular location along the height above the sea level. The wind profile can be measured using a Light Detection And Ranging (LIDAR) device [1]. LIDAR uses laser light instead of radio waves. To achieve higher accuracy it is needed that the LIDAR device stays as stationary as possible. This is done by placing the LIDAR on a stable platform or a pontoon of sorts. However, a much more economical solution is to mount the LIDAR on a floating buoy that can be relocated at wish. The goal of this letter is to propose a design for a floatable LIDAR platform that could help in accurately recording the measurements for two differently shaped buoys. The efforts and costs to relocate the LIDAR carrying vessel must be minimized to the largest possible extent. The device will be able to operate autonomously for an extended period of time. The dynamic stability has to be taken into account if the body is subjected to sudden changes of the occurring forces [2].

NUMERICAL METHODS

Numerical methods offer an inexpensive and fast alternative to test multiple situations. The models in this letter use a combination of mesh-based and mesh-free numerical methods along with a kinematic simulator.

Owing to its capability to model large deformations, Smoothed Particle Hydrodynamics (SPH) method which is a Mesh-free Particle Method (MPM) is used in this study for modelling the waves in the water domain. This technique uses particles to discretize the domain [3, 4]. Modelling of the buoy along with the platform is done using the mesh based method - Finite Element Method (FEM) which is a lagrangian method. Both the methods are coupled using a contact algorithm [5]. The result of the coupled FE-SPH simulation will yield the movement of the holding frame of the stabilization mechanism. This is given as input to Universal Mechanism (UM). This software is a commercially available kinematic and dynamic simulation software for mechanical systems and handles the movements of the mechanisms.

WATER WAVE MECHANICS

The most important parameters to describe a wave are its wavelength λ_0, wave height H and the wave period T. The wave celerity C is defined as $C= \lambda_0/T$. The wave amplitude (a) is H/2. Representative sea state data on the Thornton Bank provided by 3E and Geo Sea are used to model the sea environment.

II. NUMERICAL WAVE TANK

A schematic representation of the modelled wave tank is shown as a summary in Figure 1. The wave tank model has: a) a flap type wave generator, known as the paddle, b) a representative domain with a length of three wavelengths, and c) an SPH-symmetry plane at the side opposite to the wave generator.

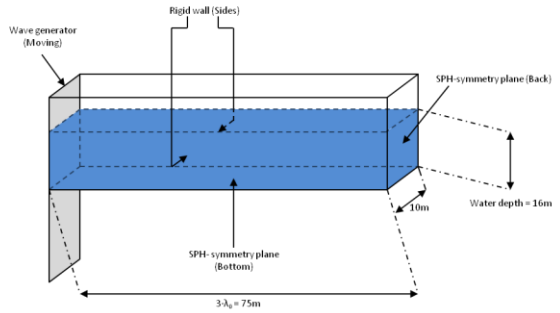

Figure 1: Boundaries and dimensions

The water in the tank is modelled using SPH particles with a particle mass of 8 kg which yields 1.5 million particles for the complete water domain with a particle volume of 0.008 m^3 or a cube of side 0.2 m. Based on the sea state data provided, a representative sea state is modelled as shown in Table 1.

Table 1: Representative sea state based wave data provided by GeoSea

Wave period T	5.594 s
Wave height H	224.46 cm
Maximum wave height H_{max}	275.69 cm
Wavelength λ_0	48.27 m

The accuracy of the wave tank model is verified by comparing these theoretical values to the simulated values. Figure 2 shows that the simulated wave data is matching the data in Table 2 quite well.

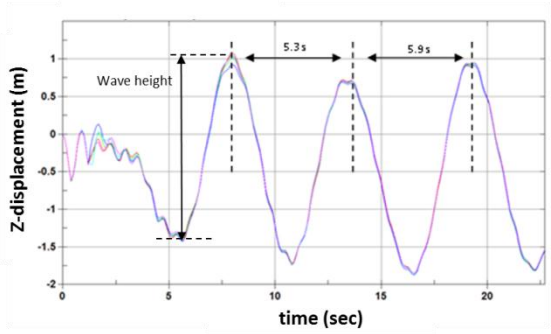

Figure 2: Wave period and Wave height

III. COMPARISON OF TWO BUOYS

Both the 3E prototype and the PEM58 buoys are simulated with the SPH wave tank. The buoys are modelled using finite elements (FE) and are assumed to be rigid. The precise mass, centre of gravity and geometry of all (sub)components have been take into account and the numerical submersion depth under gravity load has been validated. The rotations of the buoys are shown in figure 3. It clearly proves that the 3E prototype buoy gives more time for the stabilization mechanism to control the LIDAR module.

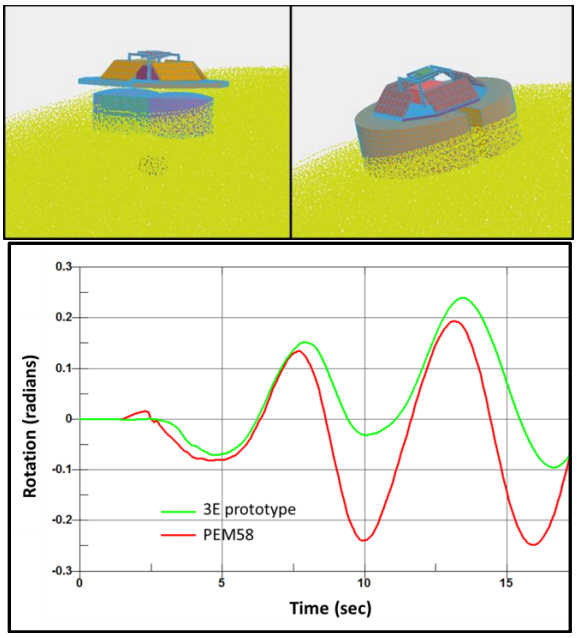

Figure 3: Comparison between the rotations of 3E and PEM58 buoys

IV. LIDAR FRAME MODEL

Since the goal is to develop a stabilization mechanism to reduce the rotations of the LIDAR module mounted on the buoy, a gyroscope based mechanism (also called gyro mechanism) is utilized in this work. Gyro mechanisms are already proven in aerospace applications [6] and a similar approach is attempted here for the floating LIDAR application. To deduce the necessary size and power requirements of the gyro mechanism and also to increase its performance a dual gimbal linkage system is designed. The movement of an inner LIDAR supporting module is made independent of the motion of the sea craft using two rotating joints. The inner frame or gimbal holding the LIDAR rotates in an outer frame or gimbal which rotates again in an external sub frame fixed to the buoy. Both axes are perpendicular to each other. The inner, and independently moving, frame with the LIDAR is stabilised by a gyroscope much smaller than the one

that would be needed to stabilise the entire craft. CAD drawings of such a linkage system which is simulated in UM are shown in figure 4(a). Figure 4(b) shows the 3E working prototype along with the FE model of the buoy and the mechanism attached to the buoy.

Initially the model is simulated in UM to test the mechanism for its stability in regular waves. Motion is described using mathematically formulated joint definitions. UM is used to simulate the mechanism. All components shown are considered to be made of steel with a density of 7800kg/m³, except for the LIDAR box which has a weight imposed. For this study, the weight of the LIDAR is taken as 45kg, which is the weight of the current LIDAR system. A stationary reference point is used in the SPH tank to measure the rotations of the buoy. These rotations are applied on the frame surrounding the LIDAR module in UM.

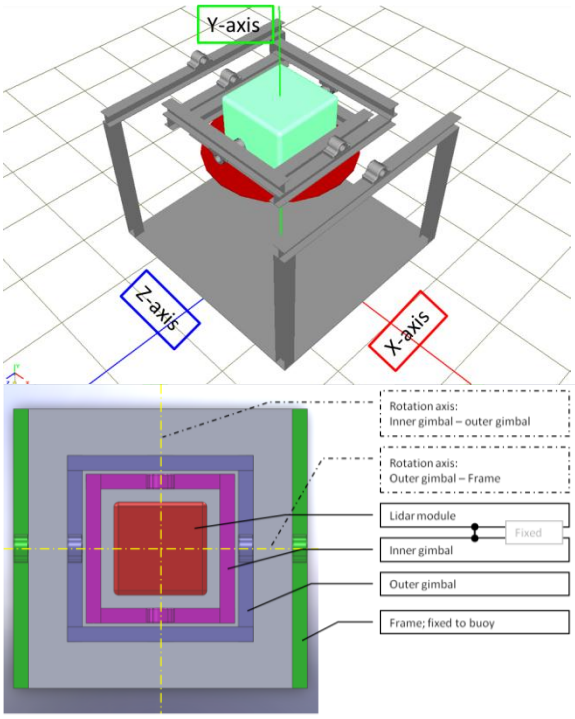

(a)

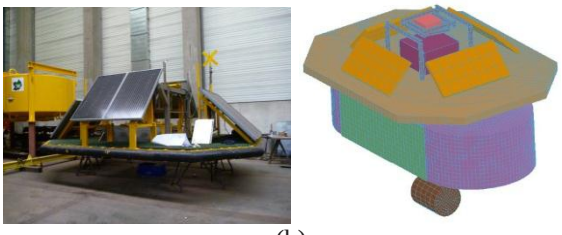

(b)

Figure 4: (a) CAD drawing of stabilization mechanism, (b) 3E working prototype and FE model

V. MECHANISM TESTING

To test the performance of the mechanism in regular waves, sinusoidal rotations are applied on the frame in X and Z directions in UM. Equation 1 gives the expression for the rotations. The rotation is expressed in radians and has a sinusoidal expression for the two rotational axes viz., X and Z shown in figure 4(a). The time variable is 't'.

$$X_i : a_i \sin\left(\frac{2\pi}{T_i} t\right) \text{ where } i = X, Z \qquad (1)$$

'a_i' is the amplitude of axis rotation and 'T_i' is the period of axis excitation. Based on measurement conditions of the LIDAR, a_i is chosen as 0.1 radians. A flywheel is placed below the mechanism and has been tested for two angular velocities 3000 rpm and 6000 rpm. These speeds are achievable with inverter fed induction motors. It may be noted here that the maximum power needed to keep a flywheel running at 3000 rpm is just 1.23 W. The rotational joints between the gimbals are very simple one degree of freedom rotational joints. An expression as shown in equation 2 is implemented defining a restoring moment $M_{restore}$ as a function of the damping coefficient C_{diss} (=20 kg.m/rad/s), relative speed v, stiffness coefficient C_{stiff} and the relative position x.

$$M_{restore} = -C_{diss}.v - C_{stiff}.x\ [Nm] \qquad (2)$$

A damping coefficient of 20 kg.m/rad/s is added to create the restoring force as a function of the relative speed and position of the joint.

As shown in figure 5, the flywheel rotational speed is inversely proportional to the maximum inclination of the LIDAR module. But beyond 6000 rpm the influence is very little.

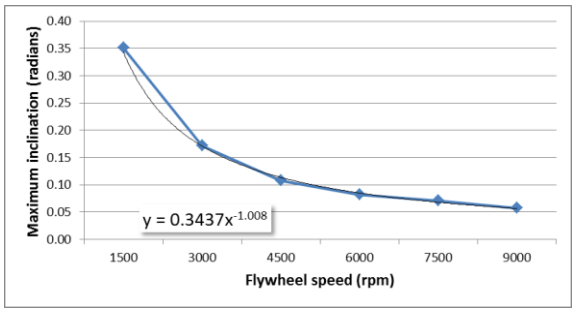

Figure 5: Influence of flywheel speed

Different diameter and thickness combinations are tested to see the influence of the flywheel and the current flywheel performs better than other combinations as shown in figure 6.

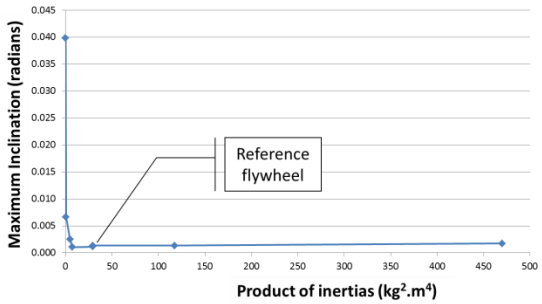

Figure 6: Influence of flywheel inertia

It is observed that the entire subsystem that must be kept upright, consisting of the LIDAR, flywheel and inner gimbal, must have its centre of gravity as closely as possible to the point around which the gimbals and outer frame rotate to prevent swaying.

VI. COUPLED SIMULATIONS

As said earlier the mechanism testing was done using simplified sinusoidal excitations. In this section, the movements of the buoy from the sea state simulations of FE-SPH are applied on the holding frame of the mechanism. This way the performance of the mechanism can be assessed when it moves in a realistic way. Finally, it will be possible to determine how accurately the LIDAR will be stabilized.

Figure 7 shows the inclination made by the LIDAR module along the direction of the waves. The LIDAR module is mounted with a gyro mechanism on both the 3E prototype and PEM58 buoys. The inclination made by the LIDAR module for three different speeds of flywheel rotation viz., 0, 3000, 6000 rpm is observed. It is clear from figure 7 that the LIDAR module on both the buoys shows not much difference in response behaviour when subjected to irregular waves with the gyro mechanism in place. It may be noted that the gyro mechanism takes care of the relatively sharper movements of the PEM58 buoy (see figure 3). Figure 7 clearly proves the point (from section V) that the stability increases with increasing flywheel speed. But changing the flywheel speed from 3000 rpm to 6000 rpm has little advantage.

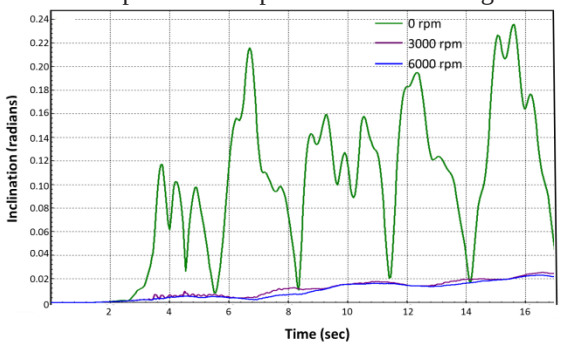

(a)

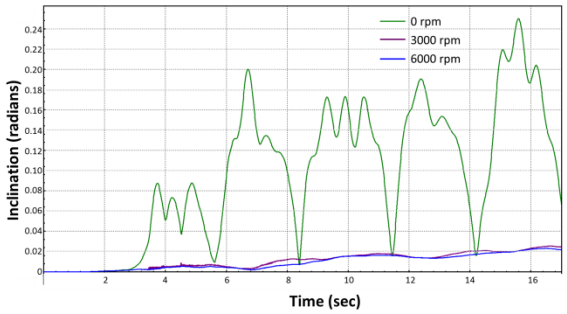

(b)

Figure 7: (a) 3E prototype and (b) PEM58 buoys in irregular waves.

VII. CONCLUSION

It can be deduced from previously discussed results and corresponding observations, that the gyroscope based LIDAR system with a flywheel not only helps in reducing the discrepancy in the results but also is easy to relocate.

It is obvious that, despite the lesser dynamic performance of the PEM58 compared to the 3E prototype as a wave filter, the results are very similar. The stabilization mechanism takes the more violent movement of the PEM58 in its stride.

VIII. ACKNOWLEDGEMENTS

The author would like to thank 3E for their support in carrying out this work. The author would also like to thank Mr. Fen Van Liefferinge and Dennis Van Eecke for their support.

IX. REFERENCES

1. Kapsali, M., J.K. Kaldellis, and S. Editor-in-Chief: Ali, *2.14 - Offshore Wind Power Basics*, in *Comprehensive Renewable Energy*, Elsevier: Oxford. p. 431-468.
2. Kim, M.H., et al., *Chapter 8 - Hydrodynamics of Offshore Structures*, in *Developments in Offshore Engineering*. 1999, Gulf Professional Publishing: Houston. p. 336-381.
3. Dalrymple, R.A. and B.D. Rogers, *Numerical modeling of water waves with the SPH method.* Coastal Engineering, 2006. **53**(2-3): p. 141-147.
4. Monaghan, J.J., *Smoothed particle hydrodynamics.* Reports on Progress in Physics, 2005. **68**(8): p. 1703-1759.
5. Groenenboom, P.H.L. and B.K. Cartwright, *Hydrodynamics and fluid-structure interaction by coupled SPH-FE method.* Journal of Hydraulic Research, 2010. **48**(sup1): p. 61-73.
6. Carnegie, C. *Gyroscopic Systems and Instruments*. 2008; Available from: http://www.allstar.fiu.edu/aero/GSI.htm.